Available online at www.sciencedirect.com
SCIENCE DIRECT®
Energy 30 (2005) 915–931
ENERGY
www.elsevier.com/locate/energy

Exergy analysis of flow dehumidification by solid desiccants

Noam Lior *, Hassan S. Al-Sharqawi [1]

Department of Mechanical Engineering and Applied Mechanics, University of Pennsylvania, 297 Towne Building, 220 South 33rd Street, Philadelphia, PA 19104-6315, USA

Abstract

Equations for the temporal and spatial exergy values and changes in the humid air stream and the desiccant for flow of humid air over desiccants and in desiccant-lined channels were established, and solved based on a thorough transient conjugate numerical analysis of laminar and turbulent flow, heat, and mass transfer that yielded the full velocity, temperature, and species concentration in the humid air and the solid desiccant. The desiccant was silica gel, the Reynolds number ranged from 333 to 3333, and the turbulence intensity in the turbulent flows was varied from 1% to 10%. Some of the major findings are: (1) in laminar flow, a total of ~20% of the humid air exergy is reduced in its drying, (2) in the desiccant, practically all of the exergy reduction is due to the release of absorption heat, (3) most of the exergy reduction, following the dehumidification rates, takes place in the first 1.5 s and first centimeter, (4) for the same inlet velocity, a desiccant-lined channel is more effective for dehumidification than a flat bed, and proportionally ~20% more exergy is expended, (5) turbulent flow improves dehumidification and proportionally increases exergy expenditure by 27–30%. Conclusions from these results are drawn to increase the exergy efficiency of the process.

1. Introduction

This paper presents an exergy analysis of the water vapor adsorption process in a desiccant–air stream system, for laminar humid air flow over a desiccant flat bed with constant and variable properties, as well as in a desiccant-lined channel, and for turbulent humid air flow in such a channel, for different turbulence intensities. The objective of the analysis is to evaluate the exergy reduction that occurs due to the adsorption and the associated heat and mass transfer processes. This knowledge is useful in guiding desiccant system design to reduce such losses and energy consumption.

* Corresponding author. Tel.: +1-215-898-4803; fax: +1-215-573-6334.
E-mail address: lior@seas.upenn.edu (N. Lior).
[1] Current address: Medina College of Technology, P.O. Box 1593, Medina, Saudi Arabia.

0360-5442/$ - see front matter © 2004 Elsevier Ltd. All rights reserved.
doi:10.1016/j.energy.2004.04.029

Nomenclature

b	thickness of silica-gel bed, m
c	specific heat, kJ/(kg K)
C	water vapor concentration, (kg water)/(kg mixture)
$\tilde{C}$	$= CM_a/M_v$
e	specific exergy, kJ/kg
E_f'''	total (average) flow exergy, kJ
E_f	local flow exergy, kJ
h	practical height perpendicular to the desiccant; channel height, m
$\bar{h}_k$	specific enthalpy of species k in the gas mixture at temperature T, J/mol
H_l	sorption heat, kJ/kg
k	species index in a gas mixture
L	length of silica-gel bed, m
m	mass, kg
M	molecular weight
m'''	water absorption rate into silica gel, kg/(s m^3)
n	number of species in a gas mixture
p	pressure, Pa
p_k	partial pressure of component k in a mixture, Pa
r	spatial direction vector
R	universal gas constant
Re_L	Reynolds number $= u_\infty L/v_f$
u	x component of velocity, m/s
$\bar{s}_k$	specific entropy of species k in the gas mixture at temperature T and partial pressure p_k of component k in the mixture, J/mol
t	time, s
TI	turbulent intensity, %
T	temperature, °C
W	water content, kg/kg
x	flow direction coordinate, m
x_a	mole fraction of the dry air in the gas mixture
x_k	the mole fraction of species k in the gas mixture
x_v	mole fraction of the water vapor in the gas mixture
y	coordinate perpendicular to x, m

Greek

σ	porosity
ρ	density, kg/m^3

Subscripts

a	air

ave	average
b	bed
ch	chemical component of the exergy
o	initial state; at the environment or "dead" state
f	fluid
th	thermo-mechanical component of the exergy
v	vapor
w	wall, i.e., the silica-gel bed
∞	free stream conditions

Superscripts

o	at the environment state
$^-$	(overbar) property is on molar basis
$'$	function only of the temperature T

The literature shows that the only past study on a related subject is that by Worek and Zheng [1], who computed the exergy losses for adsorption, purging (removing contamination from desiccant dehumidification cycle), and desorption processes that occur in an adiabatic desiccant dehumidification cycle, where the average initial and final thermodynamic states of the solid desiccant were determined from the average wall temperature and the average moisture content. They evaluated the net exergy loss in a process, which is the summation of the exergy loss of the three subprocesses. Their results revealed that the purging and desorption processes have the largest losses. Their study may be classified as a system performance study, while ours deals with the intrinsic exergy changes associated with the flow and heat and mass transfer details in the humid air and desiccant.

A conjugate transient 2D numerical solution for humid transient laminar and turbulent air flow fields over desiccant-lined finite flat plates and inside channels, including the associated heat and mass transfer phenomena was conducted here.

Some of the most relevant past studies of this problem (without the exergy analysis) are the one by Fujii and Lior [2], who numerically solved the conjugate-transient 2D heat and mass transfer problem with a steady laminar air stream passing over a thick silica-gel bed, and those by Pesaran and Mills [3,4] and Kafui [5] who treated this problem theoretically and experimentally. In their theoretical work, their model and numerical analysis were non-conjugate, i.e. the boundary conditions between the system domains were prescribed, rather than derived from the solution with the outermost boundary conditions. Pesaran and Mills [3] assumed uniform temperatures in the desiccant bed at any time, and Kafui [5] advanced the state of the art by allowing the desiccant temperature, $T(r, t)$, and water content, $W(r, t)$, to change both temporally and spatially.

In this paper, we address (1) a transient-laminar air stream passing over a flat desiccant bed 3–7 mm thick, and free stream velocities of 0.1–1 m/s, (2) a transient-laminar and turbulent air

stream in channels of 0.01–0.05 m height in which their internal walls are lined with desiccant; in the turbulent case, the problem was solved for turbulent intensities of 1–10%.

2. Model configuration

The physical system considered (Figs. 1 and 2) is a flat silica-gel-packed desiccant bed of length L with a uniform air stream passing over it in parallel. Fig. 1 shows the extended computational domain (it was extended to eliminate computational artifacts in the numerical solution, [6]) of the flat bed along the x direction, where h is the practical height in the y direction, L is the bed length, and b is the bed thickness.

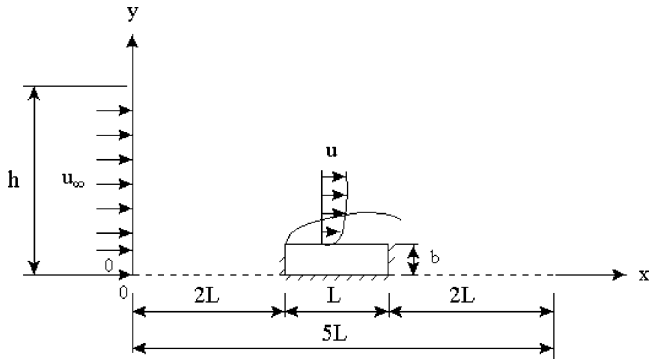

Fig. 1. The domain extended along the flow (x) direction. Note that the zone L long and b thick, is the silica-gel bed; $y = 0$ is the bottom of the bed.

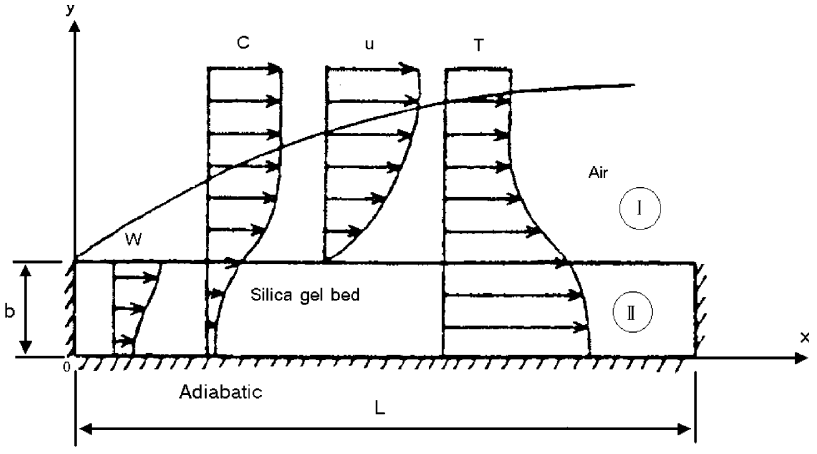

Fig. 2. The physical model configuration for the flat desiccant bed located in the extended computational domain, with a qualitative distribution depiction of the water content W, vapor concentration C, x-direction velocity u, and temperature T. Note that zone II, L long and b thick, is the silica-gel bed; $y = 0$ is the bottom of the bed.

3. The exergy equations

3.1. The derivation of equations of flow exergy for the moist air

Assuming ideal gas behavior for the air and vapor, the flow exergy per mole of mixture is (derived from [7])

$$\bar{e}_{\mathrm{f}} = \sum_{k=1}^{n} x_k \left\{ \bar{h}_k(T) - \bar{h}_k(T_{\mathrm{o}}) - T_{\mathrm{o}}\left[\bar{s}'_k(T) - \bar{s}'_k(T_{\mathrm{o}})\right] + \bar{R}T_{\mathrm{o}}\ln\left(\frac{x_k}{x_k^{\mathrm{o}}}\right) \right\} + \bar{R}T_{\mathrm{o}}\ln\left(\frac{p}{p_{\mathrm{o}}}\right) \tag{1}$$

where x_k is the mole fraction of species k in the gas mixture, $\bar{h}_k$ is the specific enthalpy of species k in the gas mixture at temperature T, $\bar{s}_k$ is the specific entropy of species k in the gas mixture at temperature T and the partial pressure ($p_k = x_k p$) of k in the mixture, T_{o} is the temperature of the environment in K, the overbar means that the property is on molar basis, the prime indicates that the entropy is a function only of the temperature T, and the o subscripts and superscripts mean that property at the environment state.

The local lost exergy is equal to entropy production rate in any part of the system, multiplied by the temperature of the environment. The entropy production rate was first prescribed by Onsager [8,9]. The force–flux relations he developed can be used to evaluate the entropy production, for instance, to obtain a consistency check on the model, but the check was not applied here and the entropy values were computed directly from the properties as described below.

Assuming the specific heats of air and water vapor, $\bar{c}_{\mathrm{pa}}$ and $\bar{c}_{\mathrm{pv}}$, are constant, Eq. (1) can be expressed as

$$\begin{aligned}\bar{e}_{\mathrm{f}} = {} & T_{\mathrm{o}}\{(x_{\mathrm{a}}\bar{c}_{\mathrm{pa}} + x_{\mathrm{v}}\bar{c}_{\mathrm{pv}})[(T/T_{\mathrm{o}}) - 1 - \ln(T/T_{\mathrm{o}})] + \bar{R}\ln(p/p_{\mathrm{o}})\} \\ & + \bar{R}T_{\mathrm{o}}[x_{\mathrm{a}}\ln(x_{\mathrm{a}}/x_{\mathrm{a}}^{\mathrm{o}}) + x_{\mathrm{v}}\ln(x_{\mathrm{v}}/x_{\mathrm{v}}^{\mathrm{o}})]\end{aligned} \tag{2}$$

To change the flow exergy expressed by Eq. (2), to a per unit mass of dry air and water vapor basis, the mole fractions x_{a} and x_{v} of dry air and water vapor, respectively, are related to the humidity ratio (water vapor concentration) C by

$$C = \frac{m_{\mathrm{v}}}{m_{\mathrm{a}}} = \frac{M_{\mathrm{v}}x_{\mathrm{v}}}{M_{\mathrm{a}}x_{\mathrm{a}}} = 0.622\frac{x_{\mathrm{v}}}{x_{\mathrm{a}}} \tag{3}$$

where m_{v} is the mass of water vapor, m_{a} is the mass of dry air, M_{v} is the molecular weight of water (=18.016), and M_{a} is the molecular weight of dry air (=28.967).

Since $x_{\mathrm{a}} + x_{\mathrm{v}} = 1$, Eq. (3) can be rearranged to give

$$x_{\mathrm{v}} = \frac{\tilde{C}}{1 + \tilde{C}} \tag{4}$$

$$x_{\mathrm{a}} = \frac{1}{1 + \tilde{C}} \tag{5}$$

where $\tilde{C} = CM_{\mathrm{a}}/M_{\mathrm{v}} = 1.6078C$.

Finally, inserting Eqs. (4) and (5) into Eq. (2), produces the following equation expressing the specific flow exergy on mass basis, (in kJ/kg)

$$e_{\mathrm{f}}(x,y) = T_{\mathrm{o}}\left\{\frac{(c_{\mathrm{pa}}+\tilde{C}(x,y)c_{\mathrm{pv}})}{(1+\tilde{C}(x,y))}\left[\left(\frac{T(x,y)}{T_{\mathrm{o}}}\right)-1-\ln\left(\frac{T(x,y)}{T_{\mathrm{o}}}\right)\right]+R\ln\left(\frac{p(x,y)}{p_{\mathrm{o}}}\right)\right\} + RT_{\mathrm{o}}\frac{1}{(1+\tilde{C}(x,y))}\left[(1+\tilde{C}(x,y))\ln\left(\frac{1+\tilde{C}^{\mathrm{o}}}{1+\tilde{C}(x,y)}\right)+\tilde{C}(x,y)\ln\left(\frac{\tilde{C}(x,y)}{\tilde{C}^{\mathrm{o}}}\right)\right] \quad (6)$$

Then, the total volume-average flow exergy (in kJ) is

$$E'''_{\mathrm{f}} = \frac{m_{\mathrm{f}}}{L(h-b)}\int_0^{(h-b)}\int_0^{L} e_{\mathrm{f}}(x,y)\,\mathrm{d}x\mathrm{d}y \quad (7)$$

where m_{f} is the mass of the moist air in the flow region and it is calculated by

$$m_{\mathrm{f}} = \rho_{\mathrm{f}}(h-b)L \quad (8)$$

where ρ_{f} is the fluid (air–water vapor) density, h is the practical height, b is the desiccant bed thickness, and L the bed length.

The local flow exergy Eq. (6) in kJ in the flow region is

$$E_{\mathrm{f}}(x,y) = e_{\mathrm{f}}(x,y)m_{\mathrm{f}}(x,y) \quad (9)$$

From Eq. (6), the volume-average thermo-mechanical and chemical components of the exergy, respectively, are

$$E'''_{\mathrm{f,\,th}} = \frac{m_{\mathrm{f}}}{L(h-b)}\int_0^{(h-b)}\int_0^{L} T_o\left\{\frac{(c_{\mathrm{pa}}+\tilde{C}(x,y)c_{\mathrm{pv}})}{(1+\tilde{C}(x,y))}\left[\left(\frac{T(x,y)}{T_{\mathrm{o}}}\right)-1-\ln\left(\frac{T(x,y)}{T_{\mathrm{o}}}\right)\right] + (1+\tilde{C}(x,y))R_{\mathrm{a}}\ln\left(\frac{p(x,y)}{p_{\mathrm{o}}}\right)\right\}\mathrm{d}x\mathrm{d}y \quad (10)$$

$$E'''_{\mathrm{f,\,ch}} = \frac{m_{\mathrm{f}}}{L(h-b)}\int_0^{(h-b)}\int_0^{L} RT_{\mathrm{o}}\frac{1}{(1+\tilde{C}(x,y))} \times\left[(1+\tilde{C}(x,y))\ln\left(\frac{1+\tilde{C}^{\mathrm{o}}}{1+\tilde{C}(x,y)}\right)+\tilde{C}(x,y)\ln\left(\frac{\tilde{C}(x,y)}{\tilde{C}^{\mathrm{o}}}\right)\right]\mathrm{d}x\mathrm{d}y \quad (11)$$

3.2. Derivation of the flow exergy of the water vapor in the desiccant bed

The amount of air that is adsorbed by desiccant is small compared to the amount of water vapor, therefore, x_{a} in Eq. (2) can be assumed to be equal to zero. Also, a term is added to Eq. (2) to represent the heat of adsorption added to the system due to absorption rate m'''.

Applying these conditions, Eq. (2) gives the specific flow exergy

$$e_{\mathrm{f,\,s}}(x,y) = T_{\mathrm{o}}\left\{c_{\mathrm{pv}}\frac{\tilde{C}(x,y)}{(1+\tilde{C}(x,y))}\left[\left(\frac{T(x,y)}{T_{\mathrm{o}}}\right)-1-\ln\left(\frac{T(x,y)}{T_{\mathrm{o}}}\right)\right]+R\ln\left(\frac{p(x,y)}{p_{\mathrm{o}}}\right)\right\} + RT_{\mathrm{o}}\frac{\tilde{C}(x,y)}{(1+\tilde{C}(x,y))}\left[\ln\left(\frac{1+\tilde{C}^{\mathrm{o}}}{1+\tilde{C}(x,y)}\right)+\ln\left(\frac{\tilde{C}(x,y)}{\tilde{C}^{\mathrm{o}}}\right)\right]-\left(\frac{H_{\mathrm{l}}m'''(x,y)}{\rho_{\mathrm{f}}}\right) \times\left(1-\frac{T_{\mathrm{o}}}{T(x,y)}\right)\Delta t \tag{12}$$

where H_{l} is the adsorption heat, m''' is the water adsorption rate, ρ_{f} is the fluid density, and Δt is the time step. Then, the total volume-average humid air exergy (in kJ) in the solid desiccant is

$$E'''_{\mathrm{f,\,s}} = \frac{m_{\mathrm{f,\,s}}}{Lb}\int_0^b\int_0^L e_{\mathrm{f,\,s}}(x,y)\mathrm{d}x\mathrm{d}y \tag{13}$$

where $m_{\mathrm{f,\,s}}$ is the mass of the fluid in the solid desiccant bed calculated by

$$m_{\mathrm{f,\,s}} = \sigma\rho_{\mathrm{f}}bL \tag{14}$$

where σ is the bed porosity.

The local flow exergy Eq. (12) is also computed in kJ at a certain location in the solid desiccant bed by

$$E_{\mathrm{f,\,s}}(x,y) = e_{\mathrm{f,\,s}}(x,y)m_{\mathrm{f,\,s}}(x,y) \tag{15}$$

From Eq. (12), the volume-average thermo-mechanical, chemical, and adsorption heat in the desiccant components of the exergy, respectively, are

$$E'''_{\mathrm{f,\,th}} = \frac{m_{\mathrm{f,\,s}}}{Lb}\int_0^b\int_0^L T_{\mathrm{o}}\left\{c_{\mathrm{pv}}\frac{\tilde{C}(x,y)}{(1+\tilde{C}(x,y))}\left[\left(\frac{T(x,y)}{T_{\mathrm{o}}}\right)-1-\ln\left(\frac{T(x,y)}{T_{\mathrm{o}}}\right)\right] +R\ln\left(\frac{p(x,y)}{p_{\mathrm{o}}}\right)\right\}\mathrm{d}x\mathrm{d}y \tag{16}$$

$$E'''_{\mathrm{f,\,ch}} = \frac{m_{\mathrm{f,\,s}}}{Lb}\int_0^b\int_0^L RT_{\mathrm{o}}\frac{\tilde{C}(x,y)}{(1+\tilde{C}(x,y))}\left[\ln\left(\frac{1+\tilde{C}^{\mathrm{o}}}{1+\tilde{C}(x,y)}\right)+\ln\left(\frac{\tilde{C}(x,y)}{\tilde{C}^{\mathrm{o}}}\right)\right]\mathrm{d}x\mathrm{d}y \tag{17}$$

$$E'''_{\mathrm{f,\,ad}} = \frac{m_{\mathrm{f,\,s}}}{Lb}\int_0^b\int_0^L\left(\frac{H_{\mathrm{l}}m'''(x,y)}{\rho_{\mathrm{f}}}\right)\left(1-\frac{T_{\mathrm{o}}}{T(x,y)}\right)\Delta t\ \mathrm{d}x\mathrm{d}y \tag{18}$$

It is noteworthy that the solid desiccant (without its vapor and air content) also has exergy, but it was not considered in this study because it depends on the temperature primarily and its variation over the small temperature range considered here is very small.

4. The model of the governing flow, heat and mass transfer, and state equations, and its solution

The calculation of the exergy, using, e.g., Eqs. (6) and (12), requires the knowledge of the transient distributions of temperature, concentration, velocities, and pressures in the flow and the desiccant. These were computed from a numerical model developed for the configurations of Figs. 1 and 2, where the fluid mechanics, energy, and species conservation equations were solved in a conjugate way, with the following assumptions:

- 2D domain.
- Flat bed and infinite-span parallel-wall channel.
- Laminar and turbulent flow.
- The turbulent flow and transport was computed using the standard k-ε model, which is known to be acceptable for the simple geometries considered in this study.
- Transient velocity, temperature, and concentration fields, with the initial conditions

$$u(x,y,0) = u_\infty \tag{19}$$

$$T(x,y,0) = T_\infty \tag{20}$$

$$C(x,y,0) = C_\infty \tag{21}$$

$$C(2L < x < 3L,\ y \le b, 0) = C_w \tag{22}$$

$$W(2L < x < 3L,\ y \le b, 0) = f(C_w, T_\infty) \tag{23}$$

- Constant properties, since their variations with the temperature in our temperature range of interest are very small. For example, in our study the temperature changes by about 4 °C, with a corresponding air specific heat change of only about 0.4%.
- No-slip boundary condition at the desiccant surface.
- Adiabatic desiccant bottom surface.
- Continuity of heat and mass flux and temperature at the fluid–solid interface.
- No heat or mass flux in the silica-gel bed in the x direction.
- Onsager-method coupling effects between heat and mass transfer are neglected because their phenomenological coefficients are very small, but the dependence of mass transfer on the temperature and of heat transfer on the species concentration are included.

The complete set of equations and the computational method are given in [2,6] and would not be repeated here. The numerical solution was by the semi-implicit method for pressure-linked equation revised (SIMPLER) algorithm control-volume method. Grid independence and convergence were examined and ensured for a grid size of 250×150 (x, y), where the computational relative error was an acceptable 10^{-4}.

As described in [6], the computational results were successfully validated by comparison to a limited amount of available experimental data from [4].

5. Results: the computed heat and mass transfer phenomena

Some of the highlights of the heat and mass transfer results are shown here, so that the exergy analysis could be understood from the process behavior fundamentals.

5.1. Laminar flow over flat desiccant bed

Fig. 3a–d show the time dependence at $x = 0.11$ m ($0.2L$ from the leading edge of the plate) of the desiccant surface water concentration, surface temperature, as well as the overall averages water content and adsorption rate for three different bed thicknesses. As expected, all of these quantities increase more rapidly at first, and then increase at a slower rate as the bed becomes increasingly water laden and thus cannot take up vapor as rapidly. The convective heat and mass transfer coefficients which dictate this behavior [6] are related to the velocity gradient $\partial u/\partial y$ through the temperature and concentration gradients in the y direction, and follow their

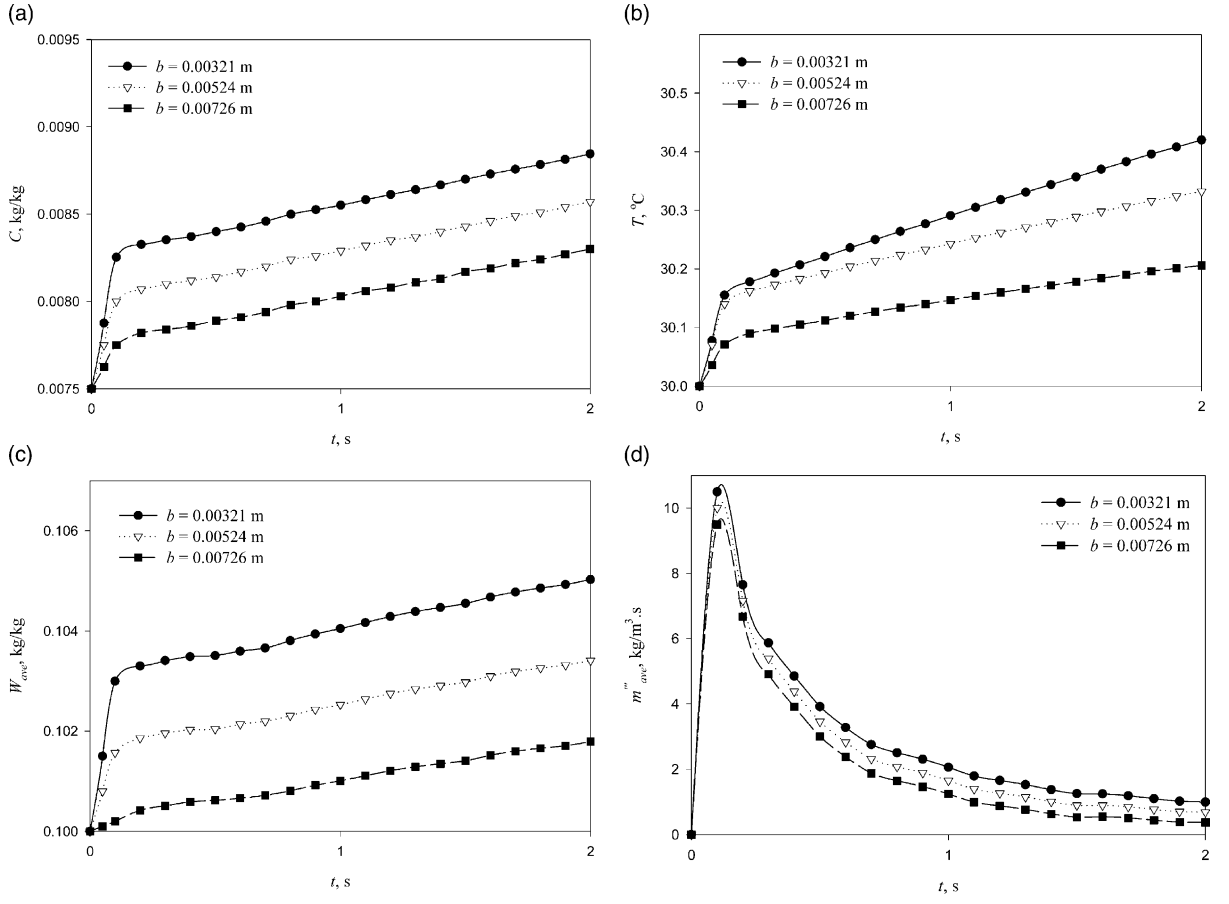

Fig. 3. Initial time dependence of desiccant (a) surface water concentration, (b) surface temperature, (c) overall average water content, and (d) overall average adsorption rate for different bed thicknesses. $u_\infty = 0.1$ m/s, $Re_L = 333$, $T_\infty = 30\ ^\circ$C, $C_\infty = 0.0276$ kg/kg, $C_b = 0.0075$ kg/kg, $W_o = 0.1$ kg/kg, $L = 0.05$ m, $h = 0.05$ m, $\sigma = 0.1$.

transient behavior. Starting with a high initial value, the convective heat and mass transfer coefficients decrease till 0.4 s, and then grow monotonically and asymptotically. Because of the local equilibrium relations, the water content exhibits a similar behavior as that of the temperature and concentration. An initial rise in the water adsorption rate occurs alongside the rapid rise in the water content. The magnitudes of the surface water concentration and the surface temperature as well as the overall averages water content and adsorption rate decrease as the bed thickness increases, due to the reduction in $\partial u/\partial y$ near the air–desiccant interface as the bed thickness increases [6].

Fig. 4a and b show the water content change with x at the desiccant surface ($y = 0.00321$ m), and with the y direction at two x positions, respectively, at $t = 20$ s. As seen in Fig. 4a, the surface water content at the bed leading edge ($x = 0.1$ m) is relatively large, again as a consequence of the large $\partial u/\partial y$ near the air–desiccant interface. The surface water content decays with x due to the corresponding reduction in $\partial u/\partial y$, which causes the reduction in mass transport coefficient. It is noteworthy here that the surface water content increases slightly near the end of the plate ($x = 0.148$–0.15 m), in the vicinity of the trailing edge ($x = 0.15$ m), due to the increase in the local mass transport coefficient there [6]. The water content inside the desiccant is seen in Fig. 4b to decrease from the bed surface down towards its bottom, and the water penetration is to higher depth at lower values of x, as expected.

5.2. Dehumidification during laminar and turbulent flow in channels

Our investigation of dehumidification in infinitely wide channel flows, where both channel walls are made of desiccant, has shown that the desiccant surface concentration, surface temperature, W_{ave}, and, m'''_{ave} behave with time very similarly to the case of the flat bed, and that increasing the channel height from 0.01 to 0.05 m reduces their values (at $t = 20$ s) by 10%, 0.9 °C, 5% and 20%, respectively. This is due to the reduction in $\partial u/\partial y$ near the air–desiccant interface as the channel height increases, which causes a reduction in the transport coefficient.

The average water content for flow in a channel is about 7% (at $t = 20$ s) higher than that over a flat bed, resulting from the fact that $\partial u/\partial y$ in the channel is 15% higher [6].

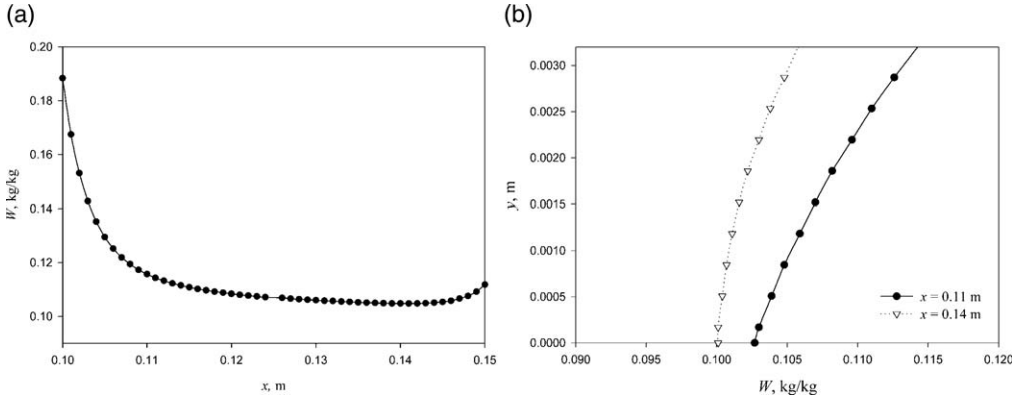

Fig. 4. Water content as functions of x and y at $t = 20$ s. $u_\infty = 0.1$ m/s, $Re_L = 333$, $T_\infty = 30$ °C, $C_\infty = 0.0276$ kg/kg, $C_b = 0.0075$ kg/kg, $W_o = 0.1$ kg/kg, $b = 0.00321$ m, $L = 0.05$ m, $h = 0.05$ m, $\sigma = 0.1$.

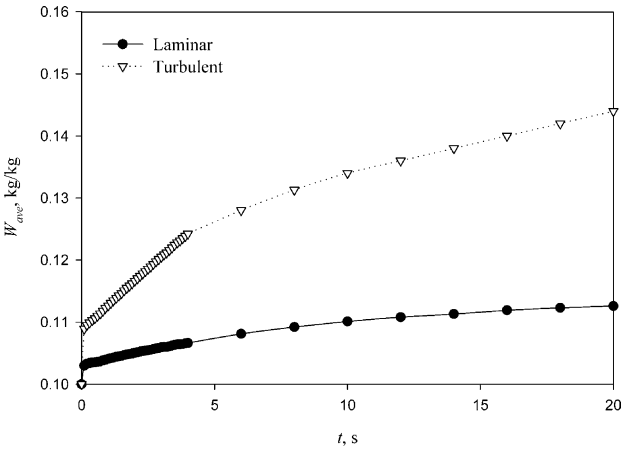

Fig. 5. Time dependence of average water content in desiccant bed for laminar and turbulent flows in channel. $u_\infty = 0.1$ m/s (laminar), $Re_L = 600$, $u_\infty = 1$ m/s (turbulent, $TI = 5\%$), $Re_t = 6000$, $T_\infty = 30\ ^\circ C$, $C_\infty = 0.0276$ kg/kg, $C_b = 0.0075$ kg/kg, $W_o = 0.1$ kg/kg, $b = 0.00321$ m, $L = 0.05$ m, $h = 0.05$ m, $\sigma = 0.1$.

It is expected that turbulent flow in channel desiccants would improve the rate of dehumidification, and, as shown in Fig. 5, increasing Re_L from 600 (laminar) to 6000 (turbulent) increases W_{ave} by 22% at $t = 20$ s, and by 10% at $t = 2$ s.

As expected, W_{ave} and m'''_{ave} were seen to increase with the turbulence intensity (TI), for example at $t = 20$ s by 7% and 20%, respectively, when the intensity is increased 10-fold, from 1% to 10%.

6. Exergy analysis results for laminar flow over a flat bed and in parallel plate channels

As explained in Section 3, the exergy was calculated from Eqs. (6), (10)–(12), and (16)–(18), using the velocity, temperature and concentration field results in the humid air flow and the desiccant, described briefly above and in more detail in [6]. Fig. 6a–b show the time dependence of average exergy the air stream and in the desiccant bed for a desiccant flat bed model with constant properties. Fig. 6a reveals that in the air stream region, the dominant component of the exergy equation (6) is the chemical one. This is due to the fact that the water vapor concentration in the flow region is 64% larger than the dead state concentration (C_o), while the temperature in the flow region is only 5 K (1.7%) larger than the dead state temperature (T_o). Therefore, the natural logarithm term in the chemical component (Eq. (11)) is much larger than that in the thermo-mechanical component (Eq. (10)), causing the chemical component to be dominant in the exergy equation (6). The average exergy drops by about 19.7% as the time increases from 0 to 1.5 s, due to the rapid increase in the water vapor concentration in the flow region with the time. After 1.5 s, the average exergy becomes nearly constant, at about 85% of the initial value, following the behavior of the concentration in the flow region.

Fig. 6b shows that in the desiccant bed, at $t = 1$ s for example, the dominant (98%) exergy component in Eq. (12) is that due to sorption heat, as compared with both the thermal (0.11%)

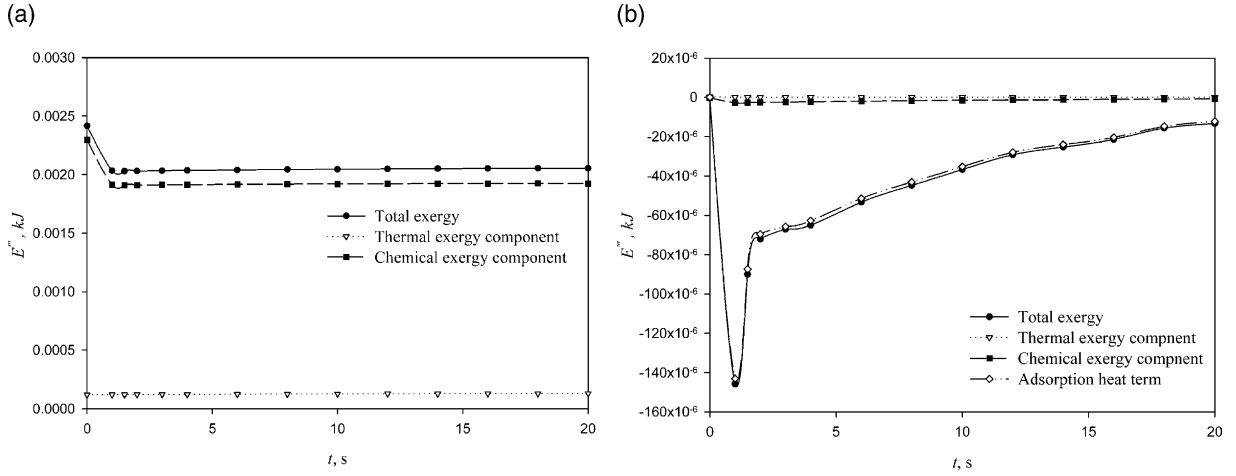

Fig. 6. Time dependence of the average value of the exergy components in (a) air stream and (b) desiccant bed. $u_\infty = 0.1$ m/s, $Re_L = 333$, $T_\infty = 30\ ^\circ$C, $C_\infty = 0.0276$ kg/kg, $C_b = 0.0075$ kg/kg, $T_o = 25\ ^\circ$C, $C_o = 0.00992$ kg/kg, $m_{f,s} = 1.9 \times 10^{-5}$ kg, $m_f = 0.0028$ kg, $b = 0.00321$ m, $L = 0.05$ m, $h = 0.05$m, $\sigma = 0.1$, $x = 0.11$ m.

and chemical (1.89%) components. The release of the sorption heat drops the total exergy of the desiccant bed from its near-zero initial value to about $-(1.45)10^{-4}$ kJ, as the water adsorption rate increases (Fig. 3), and then the exergy rises to about 90% of this value by $t = 20$ s as the adsorption rate decreases.

The total exergy in the desiccant bed is about 25-fold lower than that in the humid air stream, and the overall average exergy in the combined desiccant–air stream system is dominated by the average chemical exergy in the air stream, so the values are nearly equal to those of the air stream.

Fig. 7 shows the total exergy distributions along x in the humid air stream and desiccant bed, for several values of time. Fig. 7a shows that the local exergy in air stream near to the air–desiccant interface ($y = 0.0035$ m), where the interfacial heat and mass transport take place, first drops rapidly with x, and then arrives at a constant value. This follows the concentration trend seen in Fig. 8b. Fig. 8a shows that for $0 \leq x \leq 0.105$ m the chemical component dominates in the exergy equation (6) as compared with the thermal component because the concentration change is rapid relative to the temperature rise. The dominance reverts to the thermal component for $0.105 \leq x \leq 0.15$ m because of the reversal of the impacts of concentration and temperature in this zone. Fig. 7a also shows that the exergy of the humid air stream, say at $x = 0.11$ m, becomes almost double as the time goes from 2 to 20 s, due to the increases in the concentration in the air stream at $y = 0.0035$ m with the time (Fig. 8b). In the humid air stream at $t = 2$ and 20 s, the exergy is reduced by 81% and 70%, respectively, as x changes from 0.1 to 0.11 m. The exergy reduction thus decreases by 11% as the time increases from 2 to 20 s.

Fig. 7b shows that the local exergy in the desiccant bed near to the air–desiccant interface ($y = 0.003$ m) is more negative at the leading edge since the water adsorption rate there is large, and then it increases along the bed due to the reduction in the adsorption rate along the bed

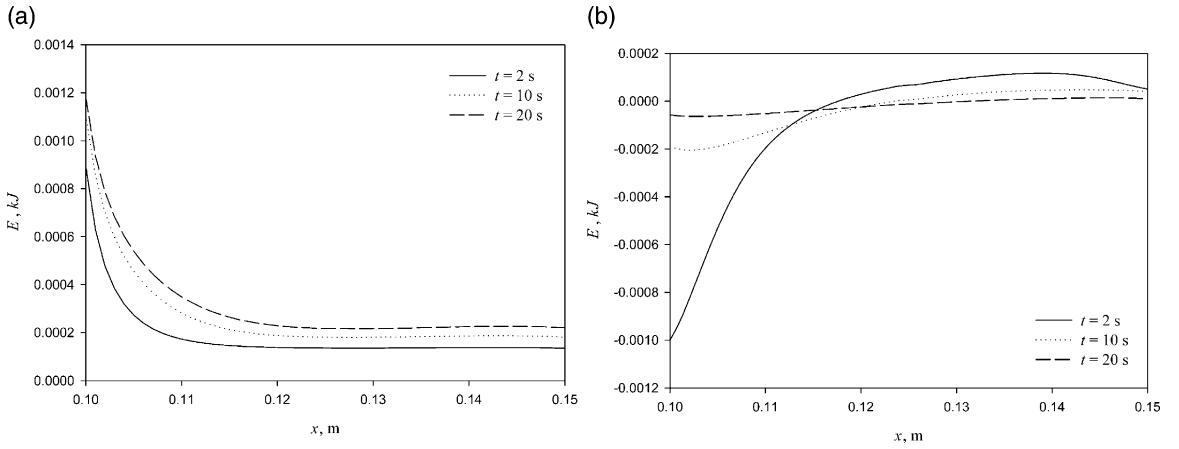

Fig. 7. Exergy distribution along the bed in (a) humid air stream and; (b) the desiccant bed for $t = 2$, 10, and 20 s. $u_\infty = 0.1$ m/s, $Re_L = 333$, $T_\infty = 30\ ^\circ$C, $C_\infty = 0.0276$ kg/kg, $C_b = 0.0075$ kg/kg, $T_o = 25\ ^\circ$C, $C_o = 0.00992$ kg/kg, $m_{f,s} = 1.9 \times 10^{-5}$ kg, $m_f = 0.0028$ kg, $b = 0.00321$ m, $L = 0.05$ m, $h = 0.05$ m, $\sigma = 0.1$.

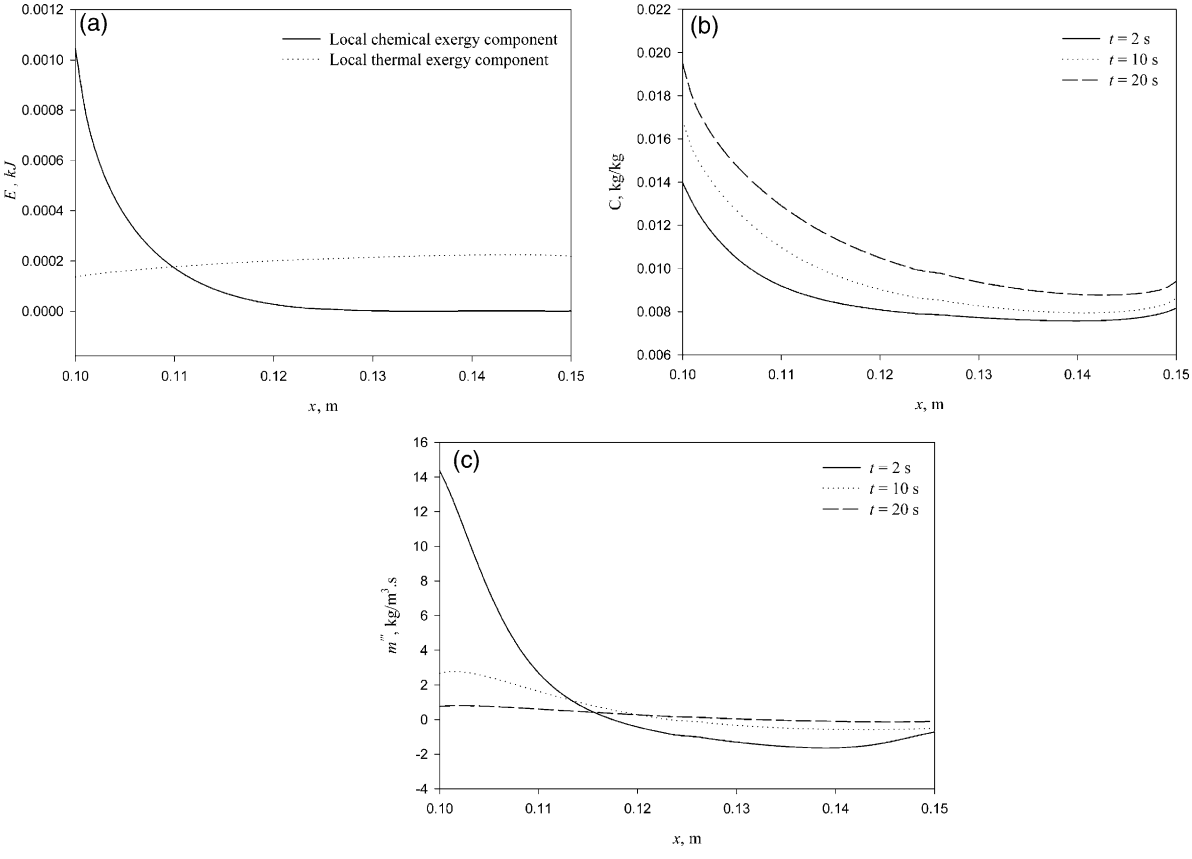

Fig. 8. (a) Exergy components, (b) water concentration, and (c) water adsorption rate distributions along the bed in the humid air stream and the desiccant bed. $u_\infty = 0.1$ m/s, $Re_L = 333$, $T_\infty = 30\ ^\circ$C, $C_\infty = 0.0276$ kg/kg, $C_b = 0.0075$ kg/kg, $T_o = 25\ ^\circ$C, $C_o = 0.00992$ kg/kg, $m_{f,s} = 1.9 \times 10^{-5}$ kg, $m_f = 0.0028$ kg, $b = 0.00321$ m, $L = 0.05$ m, $h = 0.05$ m, $\sigma = 0.1$.

(see Fig. 8c). It also shows that the exergy at say $x = 0.105$ m increases (becomes more positive) by about ninefold as the time changes from 2 to 20 s due to the reduction in the water adsorption rate with the time (Fig. 8c).

One of the exergy analysis results shown above indicates that the release of heat during the adsorption process expends exergy without any benefit. As a matter of fact, the resulting heating of the air stream being dehumidified is most often detrimental to the ultimate use of this air, such as in airconditioning applications. It was of interest therefore to determine whether this heating may not have some other effect on the exergy analysis due to the modification of the temperature-dependent properties of the desiccant. For that purpose, and to determine whether the more time-consuming computation of desiccants with variable property representation in the model is justifiable, an analysis was performed of the time dependence of the overall average exergy in desiccant–air stream system for a desiccant flat bed model with constant and variable properties as well as for a channel. Both channel walls are made of a desiccant modeled with constant properties. Fig. 9 shows that the exergy in the channel at $t = 4$ s is 2% smaller than in the flat bed with constant properties due to the higher water vapor concentration in the channel. It also shows that the exergy in the flat bed with constant properties at $t = 4$ s is about 1% smaller than that with variable properties, due to the fact that the assumption of constant properties results in a slightly higher water vapor concentration prediction. The exergy reduction in the flat bed model with variable properties is about 18.5% and it is 19.3% in the model with constant properties, as the time goes from 0 to 1 s. These minute differences between constant and variable desiccant property models indicate that the effect of variable properties is minimal, at least for this desiccant and range of conditions. The exergy reduction in the channel is about 21.4% as the time changes from 0 to 1 s.

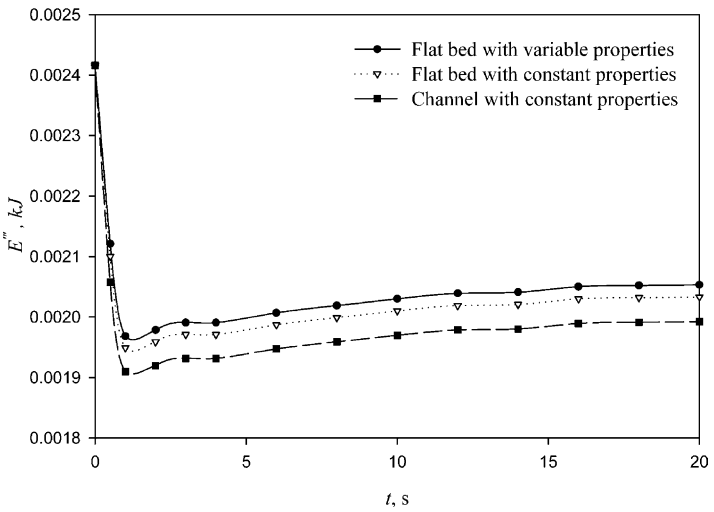

Fig. 9. Time dependence of overall average exergy in desiccant–air stream system for different cases. $u_\infty = 0.1$ m/s, $T_\infty = 30\ ^\circ$C, $C_\infty = 0.0276$ kg/kg, $C_b = 0.0075$ kg/kg, $T_o = 25\ ^\circ$C, $C_o = 0.00992$ kg/kg, $m_{f,s} = 1.9 \times 10^{-5}$ kg, $m_f = 0.0028$ kg, $b = 0.00321$ m, $L = 0.05$ m, $h = 0.05$ m, $\sigma = 0.1$.

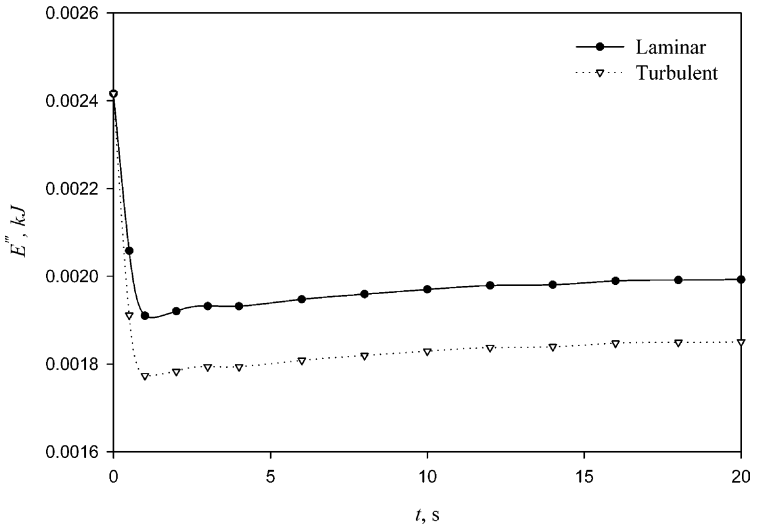

Fig. 10. Time dependence of overall average exergy in desiccant–air stream system for laminar and turbulent flows in channel. $u_\infty = 0.1$ m/s (laminar), $Re = 600$, $u_\infty = 1$ m/s (turbulent), $Re = 6000$, $T_\infty = 30\ ^\circ$C, $C_\infty = 0.0276$ kg/kg, $C_b = 0.0075$ kg/kg, $T_o = 25\ ^\circ$C, $C_o = 0.00992$ kg/kg, $m_{f,s} = 1.9 \times 10^{-5}$ kg, $m_f = 0.0028$ kg, $b = 0.00321$ m, $L = 0.05$ m, $\sigma = 0.1$.

7. Exergy analysis results for turbulent flow dehumidification in a channel

Fig. 10 shows that the exergy for the laminar flow at $t = 4$ s is about 9% larger than that for turbulent flow, due to the reduction in the water vapor concentration in the laminar flow model since the dominant component in the desiccant–air system is the chemical component in the air stream (Eq. (11)). Therefore, the overall average exergy decreases as the water vapor concentration increases with the time. The exergy reduction for laminar flow is about 19.3%, and it is 26.5% for turbulent flow, as the time goes from 0 to 1 s. While turbulence increases exergy reduction due to its dissipative nature, the main reason for the observed exergy reduction here is the increased mass transport rates due to the turbulent flow.

Fig. 11 shows the time dependence of overall average exergy in desiccant–air stream system for three turbulent intensities. Increasing the intensity 10-fold, from 1% to 10%, results in a decrease of the exergy by about 5% at $t = 4$ s. As the time goes from 0 to 1 s, the exergy reduction for 1% turbulent intensity is about 26.5%, and it is 30.3% for 10% turbulent intensity.

8. Conclusions and possible constructive uses of the exergy analysis

- In laminar flow, a total of ~20% of the humid air exergy is expended in its drying, but 90% of this is a change in chemical exergy, needed anyway; the temperature rise is $<2\ ^\circ$C.
- In the desiccant, practically all of the exergy reduction is due to the release of absorption heat, and raising the solid temperature.
- Most of the exergy reduction, following the dehumidification rates, takes place in the first 1.5 s and first centimeter.

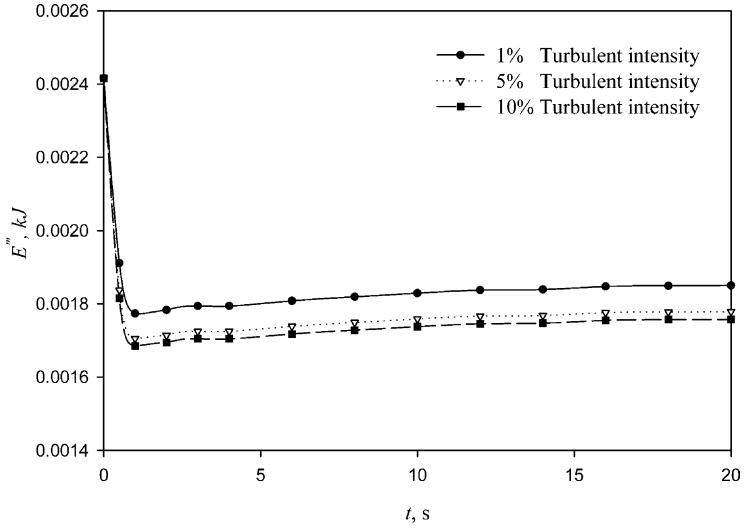

Fig. 11. Time dependence of overall average exergy in desiccant–air stream system for different turbulent intensities. $u_\infty = 1$ m/s, $Re = 6000$, $T_\infty = 30\ ^\circ$C, $C_\infty = 0.0276$ kg/kg, $C_b = 0.0075$ kg/kg, $T_o = 25\ ^\circ$C, $C_o = 0.00992$ kg/kg, $m_{f,s} = 1.9 \times 10^{-5}$ kg, $m_f = 0.0028$ kg, $b = 0.00321$ m, $L = 0.05$ m, $h = 0.05$ m, $\sigma = 0.1$.

- As the dehumidification is reduced with x, the thermo-mechanical exergy component becomes dominant, but still small.
- For the same inlet velocity, a desiccant-lined channel is more effective for dehumidification than a flat bed, and proportionally ~20% more exergy is expended.
- Turbulent flow improves dehumidification and proportionally increases exergy expenditure 27% for $TI = 1\%$ and to 30% for $TI = 10\%$.
- Desiccant dehumidification analyzed here is generally an exergy efficient process, only <7% is destroyed due to unused heating.
- Residence times beyond 1.5 s, and beds longer than 1 cm are detrimental.
- Since most of the absorption/desorption takes place near the desiccant entrance and rapidly decreases, optimal design may result from beds which are thicker at the entrance and are gradually thinned with x.
- The efficiency would be lowered for desiccants with increased heat of adsorption, flow configurations which offer low mass transfer coefficients, and those that generate higher pressure drops without commensurate increase in mass transfer coefficients.
- Synergistically with improved mass transfer coefficients, higher heat transfer coefficients improve efficiency for desiccants that have higher water uptake at lower temperatures.

Acknowledgements

The second author is grateful to the financial support of his graduate studies by his employer, The General Organization of Technical Education and Vocational Training of Saudi Arabia, the Saudi Arabian Cultural Mission in Washington, DC.

References

[1] Worek WM, Zheng W. Thermodynamic properties of adsorbed water on silica gel: exergy losses in adiabatic sorption processes. J Thermophys Heat Transfer 1991;5(3):435–40.
[2] Fujii Y, Lior N. Conjugate heat and mass transfer in a desiccant–airflow system: a numerical solution method. Numer Heat Transfer, Part A 1996;29:689–706.
[3] Pesaran AA, Mills AF. Moisture transport in silica gel packed beds-I. Theoretical study. Int J Heat Mass Transfer 1987;30(6):1037–49.
[4] Pesaran AA, Mills AF. Moisture transport in silica gel packed beds-II. Experimental study. Int J Heat Mass Transfer 1987;30(6):1051–60.
[5] Kafui KD. Transient heat and moisture transfer in thin silica gel beds. J Heat Transfer 1996;116:946–53.
[6] Al-Sharqawi HS, Lior N. Conjugate computation of transient flow and heat and mass transfer between humid air and desiccant plates and channels, paper IMECE2003-41890. Proceedings of the IMECE'03, 2003 ASME International Mechanical Engineering Congress and Exposition, Washington, DC, November 16–21. New York: ASME; 2003.
[7] Moran MJ. Availability analysis: a guide to efficient energy use. New Jersey: Prentice-Hall, Inc; 1982.
[8] Onsager L. Reciprocal relations in irreversible processes I. Phys Rev 1931;37(4):405–26.
[9] Onsager L. Reciprocal relations in irreversible processes II. Phys Rev 1931;38(12):2265–79.